



Novel coordination polymers with ferrocene-containing dicarboxylate ligand: Syntheses, crystal structures and properties

Xia Li^a, Wei Liu^b, Hong-Yun Zhang^{a,*}, Ben-Lai Wu^{a,*}

^a Department of Chemistry, Zhengzhou University, Zhengzhou 450052, PR China

^b Department of Chemistry and Chemical Engineering, Pingdingshan Engineering College, Pingdingshan 467001, PR China

ARTICLE INFO

Article history:

Received 13 May 2008

Received in revised form 24 July 2008

Accepted 29 July 2008

Available online 5 August 2008

Keywords:

Ferrocene-containing dicarboxylate

Coordination polymer

1D helical chain

Co(II) complex

Zn(II) complex

ABSTRACT

A new ferrocene-containing dicarboxylate ligand, L = 5-ferrocene-1,3-benzenedicarboxylic acid, has been prepared. Self-assembly of L, M(II) salts (M = Co and Zn) and chelating ligands dpa or phen (dpa = 2,2'-dipyridylamine and phen = 1,10-phen) gave rise to four new coordination polymers {[Co(L)(dpa)] · 2MeOH}_n (**1**), {[Zn(L)(dpa)] · 2MeOH}_n (**2**), {[Co(L)(phen)(H₂O)] · MeOH} (**3**), [Zn(L)(phen)(H₂O)] · MeOH (**4**). The isostructural complexes **1** and **2** possess 1D helical chain structures with 2₁ screw axes along the *b*-direction, and the right- and left-handed helical chains are alternate arrayed into 2D layer structures through hydrogen-bonding interactions; while isostructural complexes **3** and **4** are 1D linear chain structures with phen and ferrocene groups of L as pendants hanging on the different sides of the main chain. A structural comparison of complexes **1–4** demonstrated that the characteristics of subsidiary ligands and slight difference in coordination models of L play very important role in the construction of the complexes. In addition, the redox properties of complexes **1–4**, as well as the magnetic properties of complexes **1** and **3** are also investigated.

© 2008 Published by Elsevier B.V.

1. Introduction

Over past decades, investigation on metal-organic helical complexes has received considerable interests not only for their similarities to nucleic acids, proteins and many more natural or artificial fiber-type derivatives, but also for their potential applications in asymmetric catalysis and non-linear optical materials [1]. Although many types of metal-organic helical complexes have been reported [2], the self-assembly of helical structure is still a challenging subject due to the strenuously selection of optimal components. Recently, extensive studies have demonstrated that a good strategy for the synthesis of low-dimensional metal complex with helical structure can adopt two kinds of ligands such as non-linear V-shaped dicarboxylate ligands and aromatic bidentate chelate ligands [3].

Ferrocene and its derivatives extensively studied increasingly become an active research area since it was found in 1951 [4]. For example, coordination chemists are strongly interested in introducing ferrocene groups into a ligand framework with the objective of generating materials possessing useful electrochemical, magnetic, optical and non-linear optical properties [5]. Very recently, a new tendency is to incorporate carboxyl groups into a ferrocene backbone so as to synthesize multidentate O-donor ligands and functional metal-organic materials with high structural

diversity and stability. Up to now, numerous ferrocene-containing carboxylate complexes [6–8] have been reported, and among them, the reported ferrocenyl-based carboxylate ligands are mainly based on ferrocenecarboxylic acid [6] and 1,1'-ferrocenedicarboxylic acid [7]. However, the complexes based on ferrocene-containing aromatic dicarboxylate ligands are rarely reported.

Taking these into consideration, a V-shaped ferrocene-containing dicarboxylate ligand (L = 5-ferrocene-1,3-benzenedicarboxylic acid) has been designed and synthesized. Self-assembly of L, M(II) salts (M = Co and Zn) and chelating ligands dpa or phen (dpa = 2,2'-dipyridylamine and phen = 1,10-phen) gave rise to four new coordination polymers {[Co(L)(dpa)] · 2MeOH}_n (**1**), {[Zn(L)(dpa)] · 2MeOH}_n (**2**), {[Co(L)(phen)(H₂O)] · MeOH} (**3**), [Zn(L)(phen)(H₂O)] · MeOH (**4**). Surprisingly, among them, two polymers with dpa ligands are 1D helical chain structures as we predicted, while the other two with phen ligands do not form helices out of our prediction. To the best of our knowledge, although many helical structures have been reported, the helical structures base on ferrocene-containing carboxylate is rare. Here we want to report their preparations, crystal structures as well as electrochemical, thermal and magnetic properties.

2. Experimental

2.1. Materials and methods

All chemicals were obtained from commercial sources and used without further purification. Melting point was taken on a XT-5

* Corresponding authors. Tel.: +86 0371 67763675 (H.-Y. Zhang).

E-mail addresses: wzhy917@zzu.edu.cn (H.-Y. Zhang), wbl@zzu.edu.cn (B.-L. Wu).

microscope melting point apparatus. IR spectra were recorded on a Bruker VECTOR22 spectrophotometer with KBr pellets in 400–4000 cm^{-1} region. Element analyses were performed with a Carlo-Erba 1106 elemental analyzer. ^1H NMR spectra were recorded on a Bruker DPX-400 spectrometer in d_6 -DMSO with TMS as an internal standard. Mass spectra were measured on a LC-MSD-Trap-XCT instrument. High-resolution mass spectra were measured on a Waters Q-T of Micro spectrometer. Thermal analysis curves were scanned in a range of 30–800 $^\circ\text{C}$ with air atmosphere on STA 409 PC thermal analyzer. Differential pulse voltammetry studies were recorded with a CHI650 electrochemical analyzer utilizing the three-electrode configuration of a GC working electrode, a Pt auxiliary electrode, and a saturated calomel electrode as the reference electrode. The measurements were performed in DMF solution containing tetrabutyl ammonium perchlorate (TBAP, 0.1 mol L^{-1}) as the supporting electrolyte. DPV curves were recorded at a 20 mV s^{-1} scan rate with pulse width of 50 ms and sample width of 20 ms. The potential was scanned from +0.2 to 1.0 V. The temperature dependent magnetic measurements were determined on a Quantum Design MPMS-5 magnetometer.

2.2. Syntheses

2.2.1. 5-Ferrocene-1,3-benzenedicarboxylic acid (L)

Concentrated hydrochloric acid (20 ml) was added to a solution of 5-amino-1,3-benzenedicarboxylic acid (5.43 g, 30.0 mmol) in 60 ml water. A solution of sodium nitrite (2.21 g, 32.0 mmol) in 20 ml water was then added slowly to the tempestuously stirring mixture under a temperature range of 0–5 $^\circ\text{C}$ in an ice-bath for 20 min. The resulting diazo salt was allowed to stand for half an hour before urea was employed to get rid of the excessive sodium nitrite. Then the pale yellow thick solution was added to a solution of ferrocene (5.58 g, 30.0 mmol) in diethyl ether (60 ml) with hexadecaniltrimethylammonium bromide (0.15 g, 0.5 mmol) as a phase transfer catalysis, and the reaction mixture was allowed to react for 4 h under 10 $^\circ\text{C}$. Removing all the diethyl ether from the mixture, the deposit was gathered and adjusted to a pH value of 13 by the addition of sodium hydroxide solution (8.0%). Filtering to remove the superfluous ferrocene, the resultant dark-red solution was modulated with concentrated HCl to a pH value of 2, and then the solution was cooled to produce crude solid product which was purified by recrystallization in the methanol/water mixing solvent (3:2). Finally, the orange crystals of pure 5-ferrocene-1,3-benzenedicarboxylic acid L (yield: 45%) was obtained. HRMS: Calc. for $\text{C}_{18}\text{H}_{14}\text{FeO}_4$ $[\text{M}]^+$: 350.0242, found: 350.0255; IR (KBr, cm^{-1}): 3430 m, 1704 vs, 1601 m, 1410 m, 1279 s; ^1H NMR (400 MHz) δ ppm (DMSO): 13.32 (2H, s, –COOH), 8.30 (1H, s, –ArH), 8.24 (2H, s, –ArH), 4.90 (2H, s, –Fc), 4.44(2H, s), 4.05 (5H, s, –Fc); ESI-MS: $[\text{M}]^+$: 350.1.

2.2.2. $\{[\text{Co}(\text{L})(\text{dpa})] \cdot 2\text{MeOH}\}_n$ (1)

A methanol solution (5 ml) of dpa (0.0198 g, 0.1 mmol) was added dropwise to an aqueous solution (5 ml) of $\text{Co}(\text{NO}_3)_2 \cdot 6\text{H}_2\text{O}$ (0.0298 g, 0.1 mmol), and then a methanol solution (10 ml) of L (0.035 g, 0.1 mmol) was added slowly to the above mixture solution. Finally, the pH value of the mixture was adjusted to about 7 with NaOH aqueous solution, and the resulting orange solution was allowed to slowly evaporate at ambient temperature. Two weeks later, dark-red block crystals suitable for X-ray single crystal diffraction analysis were obtained in 56% yield based on Co. Anal. Calc. for $\text{C}_{30}\text{H}_{29}\text{CoFeN}_3\text{O}_6$: C, 56.09; H, 4.55; N, 6.54. Found: C, 55.86; H, 4.50; N, 6.42%. IR (KBr, cm^{-1}): 3422 m, 3088 m, 1634 m, 1570 s, 1479 s, 1429 m, 1371 s, 1235 m, 1160 m, 1104 m, 1013 m, 773 m, 732 m, 495 m.

2.2.3. $\{[\text{Zn}(\text{L})(\text{dpa})] \cdot 2\text{MeOH}\}_n$ (2)

A methanol solution (10 ml) of dpa (0.0198 g, 0.1 mmol) was added dropwise to a methanol solution (5 ml) of $\text{Zn}(\text{NO}_3)_2 \cdot 6\text{H}_2\text{O}$ (0.0295 g, 0.1 mmol), and then a methanol solution (10 ml) of L (0.035 g, 0.1 mmol) was added to the above mixture solution. With triethylamine slowly diffusing into the mixture for a month, orange block crystals suitable for X-ray single crystal diffraction analysis were obtained in 47% yield based on Zn. Anal. Calc. for $\text{C}_{30}\text{H}_{29}\text{FeN}_3\text{O}_6\text{Zn}$: C, 55.54; H, 4.51; N, 6.48. Found: C, 56.02; H, 4.48; N, 6.35%. IR (KBr, cm^{-1}): 3427 m, 3090 m, 1624 m, 1584 s, 1481 s, 1433 s, 1368 s, 1236 m, 1160 m, 1024 m, 774 m, 732 m, 494 m.

2.2.4. $\{[\text{Co}(\text{L})(\text{phen})(\text{H}_2\text{O})] \cdot \text{MeOH}\}_n$ (3)

A mixture of $\text{Co}(\text{NO}_3)_2 \cdot 6\text{H}_2\text{O}$ (0.0295 g, 0.1 mmol), phen (0.0198 g, 0.1 mmol), L (0.1 mmol), NaOH (0.2 mmol), MeOH (5 ml) and water (5 ml) was sealed in a 15-ml Teflon-lined stainless steel reactor. The reactor was heated in an oven to 90 $^\circ\text{C}$ for 24 h and then slowly cooled to room temperature. Red needle-shaped crystals were collected and dried in air (yield 63% based on Co). Anal. Calc. for $\text{C}_{31}\text{H}_{26}\text{CoFeN}_2\text{O}_6$: C, 58.42; H, 4.11; N, 4.40. Found: C, 57.53; H, 4.02; N, 4.24%. IR (KBr, cm^{-1}): 3421 s, 3096 m, 1613 s, 1563 s, 1448 s, 1396 s, 1107 m, 1041 m, 856 m, 828 m, 781 m, 730 s, 497 m.

2.2.5. $\{[\text{Zn}(\text{L})(\text{phen})(\text{H}_2\text{O})] \cdot \text{MeOH}\}_n$ (4)

The complex **4** was prepared using the method similar to that for complex **2** except that dpa was replaced by phen. Orange block crystals suitable for X-ray single crystal diffraction analysis were obtained in 42% yield based on Zn. Anal. Calc. for $\text{C}_{31}\text{H}_{26}\text{FeN}_2\text{O}_6\text{Zn}$: C, 57.83; H, 4.07; N, 4.35. Found: C, 57.15; H, 3.96; N, 4.28%. IR (KBr, cm^{-1}): 3429 s, 3080 m, 1628 s, 1582 s, 1429 s, 1353 s, 1103 m, 847 m, 782 m, 725 s, 492 m.

2.3. X-ray structure determination

Crystallographic data for the title compounds was collected at 291(2) K on a Bruker SMART APEX-II CCD diffractometer equipped with a graphite crystal and incident beam monochromator using Mo $\text{K}\alpha$ radiation ($\lambda = 0.71073$ Å). Absorption corrections were applied by using SADABS. The structures were solved with direct methods and refined with full-matrix least-squares techniques on F^2 using the SHELXTL program package [9]. All of the non-hydrogen atoms were refined anisotropically. The hydrogen atoms were assigned with common isotropic displacement factors and included in the final refinement by using geometrical restraints. Crystal data are summarized in detail in Table 1. Selected bond lengths and bond angles are listed in Table 2.

3. Results and discussion

3.1. Synthesis

The main ligands in all complexes are L and secondary ligands dpa and phen are very similar, but the synthesis methods of **1–4** are very different. Complex **1** was obtained through the slow evaporation of solvent. Due to easily depositing under the similar condition of **1**, compounds **2** and **4** created from the slow diffusion of triethylamine into the reaction systems. However, complex **3** was synthesized through the hydrothermal method due to easily forming polycrystal under the similar condition of **1**. As reported in literature, most of the ferrocene-containing complexes are sensible for light. However, the 5-ferrocene-1,3-benzenedicarboxylic acid ligand and the corresponding complexes **1–4** are very stable under the light and high temperature and pressure, which make them be more easily handled in potential application. All of the complexes

Table 1
Crystal data and structure refinement for complexes 1–4

Complex	1	2	3	4
Formula	C ₃₀ H ₂₉ CoFeN ₃ O ₆	C ₃₀ H ₂₉ FeN ₃ O ₆ Zn	C ₃₁ H ₂₆ CoFeN ₂ O ₆	C ₃₁ H ₂₆ FeN ₂ O ₆ Zn
Formula weight	642.34	648.78	637.32	643.76
Crystal system	Monoclinic	Monoclinic	Triclinic	Triclinic
Space group	P2 ₁ /c	P2 ₁ /c	P $\bar{1}$	P $\bar{1}$
a (Å)	10.478(2)	10.549(2)	9.6959(12)	9.7240(19)
b (Å)	11.196(2)	11.073(2)	10.0016(12)	10.214(2)
c (Å)	24.220(5)	24.245(5)	14.2310(18)	14.320(3)
α (°)	90	90	94.555(2)	93.32(3)
β (°)	93.43(3)	94.58(3)	102.563(2)	103.32(3)
γ (°)	90	90	92.556(2)	92.87(3)
V (Å ³)	2836.2(10)	2823.2(10)	1340.0(3)	1378.7(5)
Z	4	4	2	2
D _{calc} (g/cm ³)	1.504	1.526	1.580	1.551
F(000)	1324	1336	654	660
θ range (°)	2.00–25.50	3.08–25.49	2.41–26.00	2.31–26.00
Index range (°)	–12 ≤ h ≤ 11, –13 ≤ k ≤ 13, –26 ≤ l ≤ 29	–12 ≤ h ≤ 12, –13 ≤ k ≤ 13, –29 ≤ l ≤ 29	–11 ≤ h ≤ 11, –12 ≤ k ≤ 12, –17 ≤ l ≤ 17	–11 ≤ h ≤ 11, –12 ≤ k ≤ 12, –17 ≤ l ≤ 17
Reflections collected/unique [R _{int}]	15407/5263 [0.0175]	29115/5250 [0.0497]	10453/5219 [0.0291]	10929/5351 [0.0407]
Goodness-of-fit on F ² (GOF)	1.048	1.177	1.080	0.981
R ₁ , wR ₂ (I > 2σ(I))	0.0395, 0.1057	0.0593, 0.1357	0.0450, 0.1155	0.0452, 0.0918
R ₁ , wR ₂ (all date)	0.0480, 0.1110	0.0674, 0.1404	0.0680, 0.1267	0.0845, 0.1071
Largest difference in peak and hole (e Å ^{–3})	0.706, –0.657	0.656, –0.637	0.348, –0.612	0.508, –0.397

Table 2
Selected bond distances (Å) and angles (deg) for polymers 1–4

1					
Co1–N3	2.032(2)	Co1–O3	2.039(2)	Co1–O1	2.0466(19)
Co1–N1	2.063(3)	Co1–O2	2.285(2)		
N1–Co1–O2	154.59(9)	N3–Co1–O3	138.92(10)	N3–Co1–O1	117.04(9)
O3–Co1–O1	102.24(9)	N3–Co1–N1	91.01(10)	O3–Co1–N1	97.58(9)
O1–Co1–N1	94.72(9)	N3–Co1–O2	97.62(9)	O3–Co1–O2	91.52(9)
O1–Co1–O2	60.08(7)				
2^a					
Zn1–O2	1.973(3)	Zn1–O4A	2.020(3)	Zn1–N1	2.022(3)
Zn1–N3	2.068(3)	Zn1–O3A	2.403(3)		
O4–Zn1B	2.020(3)	O3–Zn1B	2.403(3)		
O2–Zn1–O4A	109.14(12)	O2–Zn1–N1	28.78(13)	O4A–Zn1–N1	117.76(13)
O2–Zn1–N3	102.56(13)	O4A–Zn1–N3	96.57(13)	N1–Zn1–N3	91.80(13)
O2–Zn1–O3A	90.73(12)	O4A–Zn1–O3A	8.24(11)	N1–Zn1–O3A	96.72(12)
N3–Zn1–O3A	154.49(12)				
3					
Co1–O3	2.091(2)	Co1–O5	2.096(3)	Co1–O2	2.101(3)
Co1–N1	2.133(3)	Co1–N2	2.167(3)		
O3–Co1–O5	99.79(11)	O3–Co1–O2	87.80(10)	O5–Co1–O2	89.93(12)
O3–Co1–N1	132.16(10)	O5–Co1–N1	96.67(11)	O2–Co1–N1	136.92(10)
O3–Co1–N2	88.54(11)	O5–Co1–N2	171.56(11)	O2–Co1–N2	91.82(11)
N1–Co1–N2	76.47(11)				
4					
Zn1–O2	2.027(3)	Zn1–O3	2.080(3)	Zn1–O5	2.098(3)
Zn1–N2	2.151(3)	Zn1–N1	2.227(3)		
O2–Zn1–O3	96.14(11)	O2–Zn1–O5	98.35(11)	O3–Zn1–O5	90.68(11)
O2–Zn1–N2	124.37(11)	O3–Zn1–N2	137.97(11)	O5–Zn1–N2	93.63(12)
O2–Zn1–N1	92.48(12)	O3–Zn1–N1	93.43(11)	O5–Zn1–N1	167.95(12)
N2–Zn1–N1	75.78(11)				

^a Symmetry transformations used to generate equivalent atoms: A, $-x + 1, y - 1/2, -z + 1/2$; B, $-x + 1, y + 1/2, -z + 1/2$.

are insoluble in common solvent, such as MeOH, EtOH, MeCN and THF. To our knowledge, most of the reported ferrocene-containing carboxylate complexes are based on the d¹⁰ metal centers (Zn, Cd and Pb etc.), and few of those polymers contain Co metal centers [7b].

3.2. Structure description

Because complexes **1** and **2** are isostructural, and **3** and **4** are also isostructural, only the structures of **1** and **3** are discussed in

detail for terseness. The coordination environments around metal centers of complexes **2** and **4** as Supporting information are given.

3.2.1. {[Co(L)(dpa)] · 2MeOH}_n (**1**)

A single crystal XRD study has revealed that complex **1** crystallizes in a space group P2₁/c and has 1D helical chains. As shown in Fig. 1, each five-coordinate Co(II) center is in a seriously distorted trigonal bipyramid geometry, defined by two nitrogen atoms (N1, N3) of dpa and three oxygen atoms (O1, O2 and O3) from carboxyl group of two different L. Atoms N1, O1 and O2 form an equatorial plane (the

deviation of center Co atom from the mean plane is about 0.0268 Å, while atoms O3 and N3 occupy the axial position. The bond angle of O1–Co–N3 is 138.93°. The Co–O distances range from 2.039(2) to 2.285(2) Å, while Co–N distances are 2.032(2) and 2.063(3) Å, respectively, which is close to the related Co(II) coordination polymers $\text{Co}_2(\text{O}_2\text{CfcCO}_2)_2(2,2'\text{-bpy})_2(\mu_2\text{-OH}_2)_2 \cdot \text{CH}_3\text{OH} \cdot 2\text{H}_2\text{O}$ [7b], $[\text{Co}(\text{Pht})(\text{bpy})(\text{H}_2\text{O})_3] \cdot 3\text{H}_2\text{O}$ [10] and $[\text{Co}(\text{PCPA})(\text{IN})]_n$ [11].

The dihedral angle between the carboxyl groups and the phenyl ring are 166.2° and 71°, respectively. A visible twisting is observed between the Cp ring and the phenyl ring to which is attached, with the dihedral angle between them being 161.5°. No significant deformation of the almost parallel Cp ring is observed. In each dpa, the average deviation of the whole molecular plane is 0.0661 Å, and the dihedral angle between two pyridine rings is 7.9°.

Each ligand L serving as a bisconnector through its two carboxyl moieties bridges two Co atoms to afford an infinite 1D chain. There exist two different coordination modes of the two carboxyls: monodentate and chelate coordinations. The distance of adjacent Co atoms separated by L is 9.16(9) Å. Notably the 1D chain structure is a helix with a pitch of 11.19(6) Å following a 2_1 screw axis along the *b*-direction (Fig. 1). The dpa ligands are alternately attached to both sides of the single-stranded helical chain. Two adjacent helical chain with different handedness are bridged by two types of hydrogen-bonds: one is $\text{N2-H2A} \cdots \text{O6}$ formed by the uncoordinated amino hydrogen atom of dpa and the oxygen atom of lattice methanol molecule, and the other is $\text{O6-H11} \cdots \text{O3}$ formed by the lattice CH_3OH hydrogen atom and the coordinated O atoms of the monodentate carboxyl group. The N2–O6 and O6–O3 distances are 2.885(3) and 2.837(3) Å, respectively. As a result of the alternate arrangement of the right- and left-handed helical chains through interchain hydrogen-bonding interactions, a 2D mesomeric layer is fabricated (Fig. 2). To the best of our knowledge, although a lot of helical structures have been reported, the helical chain structures based on ferrocene-containing carboxylate are extremely rare. In addition, the dpa ligands between the adjacent helical chains are par-

allel with the separation of 3.80(6) Å, indicating weak π - π stacking interactions, which makes the solid state structure more stable.

3.2.2. $\{[\text{Co}(\text{L})(\text{phen})(\text{H}_2\text{O})] \cdot \text{MeOH}\} (\mathbf{3})$

The crystal structure analysis by X-ray diffraction demonstrates that complex **3** crystallized in a space group $P\bar{1}$. As shown in Fig. 3, each Co(II) is also five-coordinated and located in a distorted trigonal bipyramid geometry ligated by two nitrogen atoms from phen, two oxygen atoms from two different carboxylate of L and one oxygen atoms from coordinated water molecule. The O2, O3 and N1 atoms form an equatorial plane (the deviation of center Co atom from the mean plane is about 0.0756 Å), and O5 and N2 occupy the axial position (O5–Co1–N2 171.56(11)°). The Co–O distances range from 2.091(2) to 2.101(3) Å, which is consistent with those in complex **3**, while the Co–N distances of 2.133 and 2.1671 Å are slightly longer than those found in **3**.

The phenyl ring and the cyclopentadienyl (Cp) are almost coplanar with the mean deviation from the plane being 0.0566 Å. The two carboxylate groups have 5.4° and 158.7° dihedral angles with the plane of corresponding linking phenyl rings, respectively. It is clear that the phen ring is almost perpendicular to the plane of correspondingly linked phenyl ring, and the dihedral angle between them is 93.3°. No significant deformation of the almost parallel Cp ring is observed.

In **3**, each L adopt a bis(monodentate) coordination mode and acts as a μ_2 -bridge linking two Co atoms to give an one-dimensional linear chain. The distance of two adjacent Co atoms separated by L is 10.00(2) Å, which is slightly longer than that in **1**. The ferrocene and phen hang on the different sides of the main chain with phen rings or cp rings paralleling each other, respec-

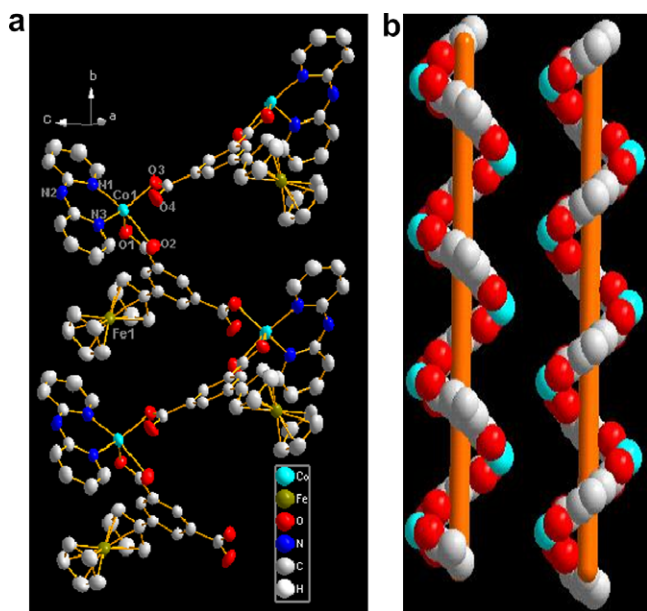


Fig. 1. (a) ORTEP drawing with heteroatom labeling scheme of 1D helical chain structure of $\{[\text{Co}(\text{L})(\text{dpa})] \cdot 2\text{MeOH}\}_n$ (**1**) (H atoms and uncoordinated solvent molecules are omitted for clarity). (b) Space-filling model of left-handed (left) and right-handed (right) helical chains (H, Fe group and part of dpa atoms are omitted for clarity).

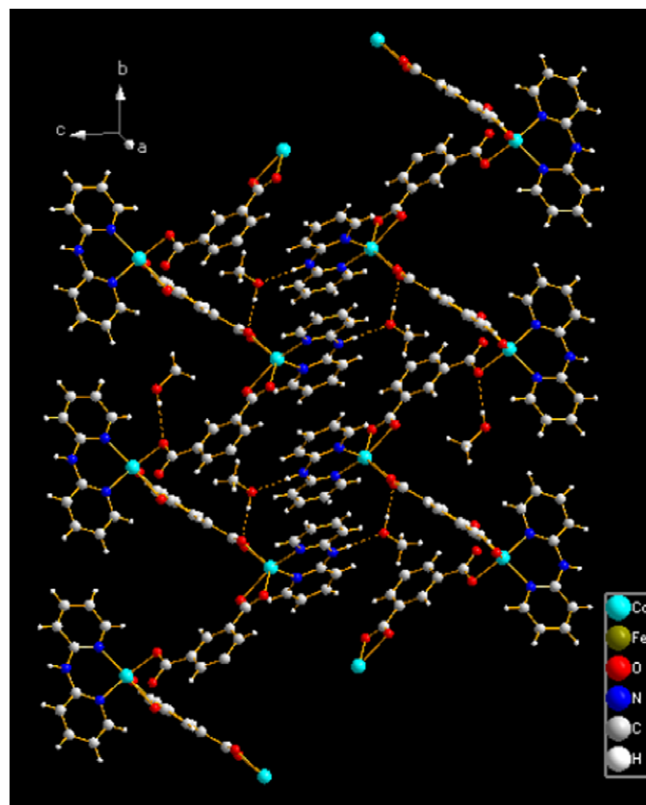


Fig. 2. View of 2D supramolecular network in **1** forming through hydrogen-bond interactions alternately linking the right- and left-handed helices. The hydrogen-bonding interactions between the chains are indicated as ... (Fc group was omitted for clarity).

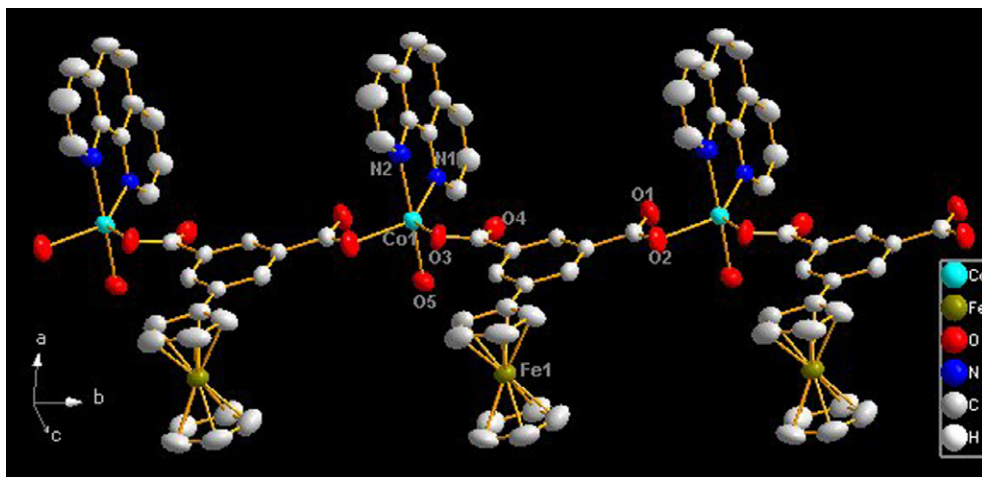


Fig. 3. ORTEP drawing with heteroatom labeling scheme of 1D lineal chain structure of $[\text{Co}(\text{L})(\text{phen})(\text{H}_2\text{O})] \cdot \text{MeOH}$ (**3**) (H atoms and uncoordinated solvent molecules are omitted for clarity).

tively. The separations between the adjacent Co atoms, Fe atoms and phen rings are all $10.00(2) \text{ \AA}$. At opposite positions the adjacent linear chains are further bridged to form a parallel double chains through different $\text{O}-\text{H} \cdots \text{O}$ ($\text{O}-\text{H} \cdots \text{O} = 2.673\text{--}2.733 \text{ \AA}$, $\angle \text{O}-\text{H} \cdots \text{O} = 165\text{--}176^\circ$) hydrogen-bond interactions, originating from the coordinated water hydrogen atoms and lattice CH_3OH hydrogen atoms, respectively, to the uncoordinated oxygen of the carboxylate group, or from the coordinated water hydrogen atoms to the lattice CH_3OH oxygen atoms (Fig. 4). Moreover, the double chains are further extended to a layer network through the aromatic π - π stacking interactions of the phen groups between the adjacent layers (Fig. 5), and the closest distance between adjacent aromatic rings is $3.32(2) \text{ \AA}$.

Comparing the structures of **1–4**, it is easy to conclude that changing the subsidiary ligands may affect the architecture of the complexes. In contrast to phen, although they are both chelating ligands, dpa with an excess amino-N atom displays more lability and plentiful hydrogen-bonding interactions. Moreover, the bite angles ($\angle \text{N}-\text{M}-\text{N}$) of dpa and phen are very different, 91.0° and 91.8° for **1** and **2**, 76.5° and 75.8° for **3** and **4**, respectively, maybe which is the most important reason why the complexes based on dpa are easily to form a 1D helical chain. Further, the packing interactions in **1–4** are different. The 2D supramolecular network of complexes **1** and **2** are mainly supported by the hydrogen-bonding of dpa, while **3** and **4** are mainly supported by the π - π stacking interaction of phen. Moreover, in complexes **1** and

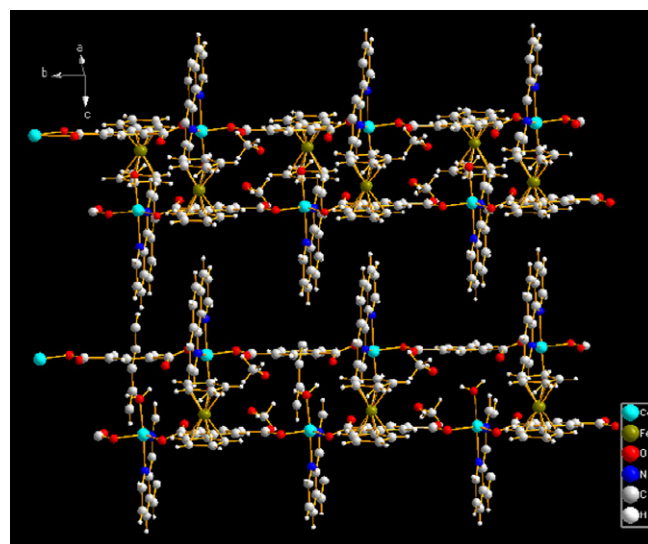


Fig. 5. 2D network of **3** showing the π - π stacking interactions between phen.

2 the two-connectors L link metal nodes with one carboxylate monodentate coordination and the other chelate coordination whereas in complexes **3** and **4** ligands L only act as bis(monoden-

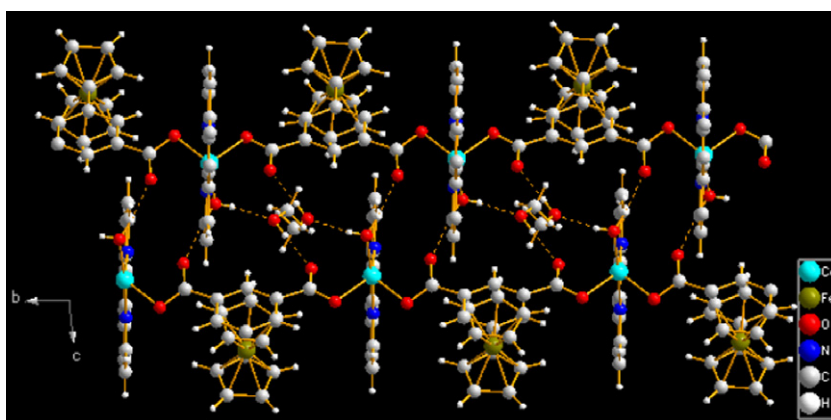


Fig. 4. The double linear chains bridged by the hydrogen-bonding in complex **3**. The hydrogen-bonding interactions between the chains are indicated as ...

tate) bridges, and the slight difference in coordination models may play a key role in the architectural variation.

3.3. IR spectroscopy

The IR spectra of complexes **1** and **2** are similar, while those of complexes **3** and **4** are also similar. The absence of absorption bands at 1731–1651 cm^{-1} where the $-\text{COOH}$ is expected to appear illustrates the complete deprotonation of L upon its coordination to metal ions. For **1**, the bands at 3087 and 495 cm^{-1} (3090 and 494 cm^{-1} for **2**, 3096 and 497 cm^{-1} for **3**, 3080 and 492 cm^{-1} for **4**) are attributed to the typical characteristic $\nu(\text{C}-\text{H})$ and $\nu(\text{Fe}-\text{Cp})$ vibration of the ferrocenyl group [12]. The strong absorption bands at 1570 and 1371 cm^{-1} (1584 and 1368 cm^{-1} for **2**, 1563 and 1396 cm^{-1} for **3**, 1570 and 1371 cm^{-1} for **4**) are due to the asymmetric $\nu_{\text{as}}(\text{COO}^-)$ and symmetric $\nu_{\text{s}}(\text{COO}^-)$ stretching vibrations. The broad bands at 3420 cm^{-1} belong to the typical band of hydroxyl group. In conclusion, the IR data are in good agreement with the X-ray analyses.

3.4. X-ray powder diffraction measurement

To confirm whether the analyzed crystal structures are truly representative of the bulk materials, X-ray powder diffraction (XRPD) experiments were carried out for complexes **1–4** at room temperature (Fig. 6). Their peak positions are in good agreement with each other, indicating the phase purity of the products. The differences in intensity may be due to the preferred orientation of the powder samples.

3.5. Thermogravimetric analysis (TGA)

To investigate their thermal stabilities, thermogravimetric analyses (TGA) of **1–4** were carried out under air atmosphere with flow rate of 60 mL min^{-1} and heating rate of 10 $^{\circ}\text{C min}^{-1}$. The TG analyses reveal that the thermal decomposition behaviors of complexes **1–4** were similar. For **1**, it is stable up to 65 $^{\circ}\text{C}$. A total weight loss of 10.24% occurred in the temperature range of 65–308 $^{\circ}\text{C}$, probably corresponding to the remove of free methanol molecules (calcd. 9.96%). The second obvious weight loss takes place from 308 to 474 $^{\circ}\text{C}$, and the weight loss is 65.79%, which is

assigned to the decomposition of ligand L and dpa groups (calcd. 65.94%). The left residue of 23.97% can be attributed to the formation of CoO and Fe_2O_3 (calcd. 24.10%). Similarly, the first decomposition step starts at 90.7, 121 and 60 $^{\circ}\text{C}$ for **2–4**, respectively, corresponding with the weight loss of 9.38%, 7.32% and 4.63%, respectively. Then the second step of weight losing takes place in the temperature range of 323–500 $^{\circ}\text{C}$ for **2**, 326–540 for **3** and 309–486 for **4**, respectively, with the sharp weight loss of 64.89% for **2**, 66.03% for **3** and 65.19% for **4**, respectively. Following continuous heating, the smooth platforms were observed.

3.6. Redox properties

The electrochemical behaviors of **1–4** and ligand L were studied by differential pulse voltammetry at a GC working electrode in DMF. Both L and the complexes show a single peak corresponding to the single-electron Fc/Fc^+ couple oxidation processes, with the half-wave potential being 560, 562, 565, 564, 571 mV for L and **1–4**, respectively. The electrochemical results show that coordinated metal ions $\text{Co}(\text{II})$ and $\text{Zn}(\text{II})$ do not affect the potential of the Fc/Fc^+ couple in polymers **1–4**. Similar condition also can be found in other reported ferrocene-containing carboxylate complexes, $\{\text{Zn}(\text{FcCOO})_2(\text{bbbm})\} \cdot 2\text{H}_2\text{O}\}_n$ [13], $[\text{Ba}(\text{OOCFcCOO})(\text{H}_2\text{O})]_n$ [7c] and $\{[\text{Pb}(\mu_2-\eta^2-\text{OOCCH}=(\text{CH}_3)\text{CFc})] \cdot \text{MeOH}\}_n$ [8a].

3.7. Magnetic properties

The temperature (T) dependencies of the magnetic susceptibility (χ_M) of complexes **1** and **3** were measured in the temperature range 2–300 K under fixed fields of 1 kOe, and the magnetic susceptibilities χ_M and μ_{eff} versus T plots are shown in Figs. 7 and 8, respectively.

For complex **1**, the experimental μ_{eff} value at room temperature is 4.91 μ_B , which is larger than the spin-only value of high-spin cobalt(II), 3.87 μ_B , indicating a typical contribution of the orbital momentum for the $4T_g^1$ ground state. Upon cooling, the μ_{eff} gradually decreases to a value of 3.71 μ_B at 2 K. As shown in the χ_M^{-1} versus T plot, all data follow the Curie–Weiss law closely with $C = 3.01 \text{ cm}^3 \text{ mol}^{-1} \text{ K}$ and $\theta = -7.86 \text{ K}$. The negative value of θ indicates weak antiferromagnetic interactions between adjacent $\text{Co}(\text{II})$ ions.

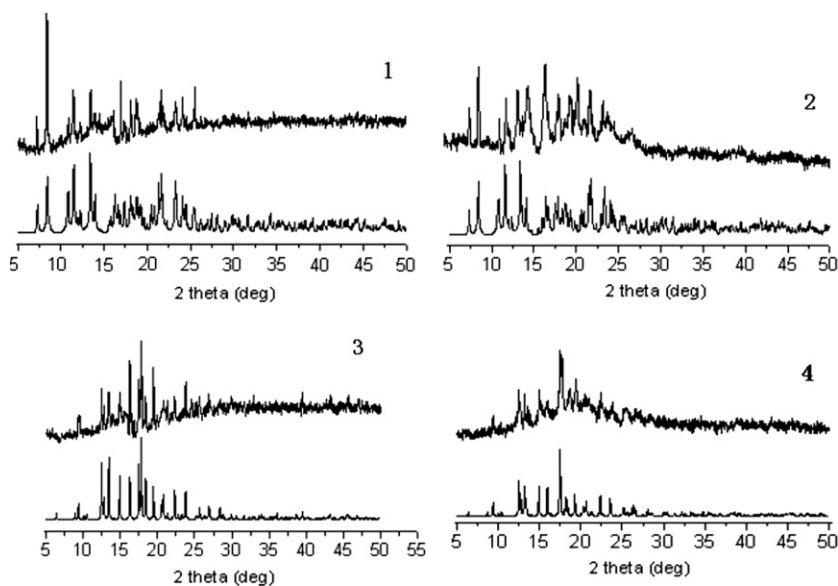


Fig. 6. XRPD patterns for complexes **1–4**: (bottom) calculated patterns from single crystal X-ray data; (top) measured patterns.

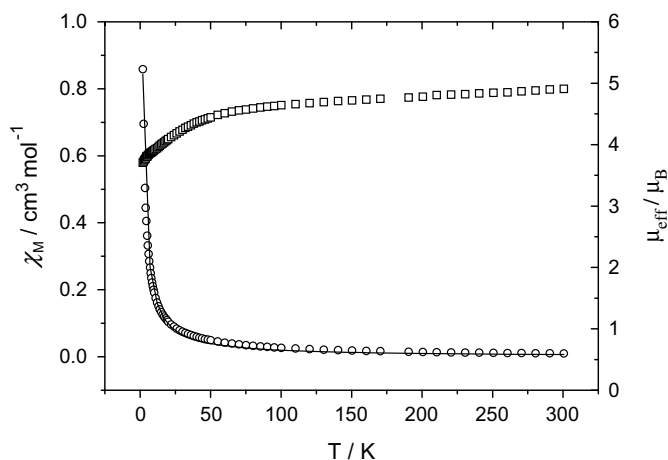


Fig. 7. χ_M (○) and μ_{eff} (□) vs. T plot with the theoretical fit (–) for **1**.

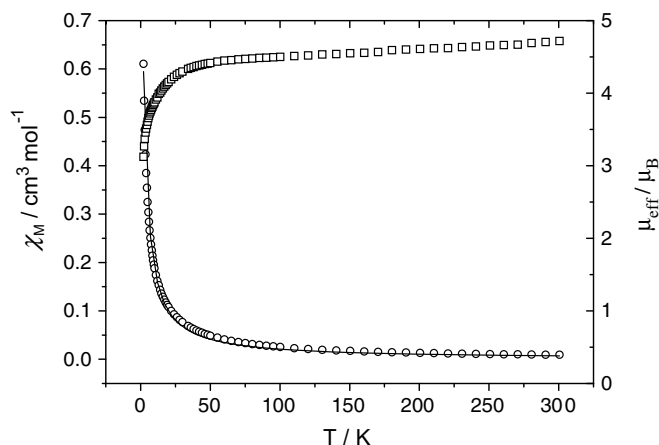


Fig. 8. χ_M (○) and μ_{eff} (□) vs. T plot with the theoretical fit (–) for **3**.

For complex **3**, the experimental μ_{eff} value at room temperature is $4.72 \mu_B$, which is larger than the spin-only value of high-spin cobalt(II), $3.87 \mu_B$, indicating a typical contribution of the orbital momentum for the $4T_1^g$ ground state. As the temperature lowered, the μ_{eff} gradually decreases to a value of $4.37 \mu_B$ at 40 K, and then decreases more rapidly at low temperatures, reaching a value of $3.12 \mu_B$ at 2 K. As shown in the χ_M^{-1} versus T plot, all data follow the Curie–Weiss law closely $C = 2.76 \text{ cm}^3 \text{ mol}^{-1} \text{ K}$ and $\theta = -5.66 \text{ K}$. The negative value of θ may be attributed to antiferromagnetic interactions between Co(II) ions.

The susceptibility data of complexes **1** and **3** can be simulated with the analytical equation (see below) reported by Hong et al. [14].

$$\chi_M = \frac{N\beta^2 g^2 S(S+1)}{3kT} \frac{1+u}{1-u} \quad (1)$$

$$\text{where } u = \coth \left[\frac{JS(S+1)}{kT} \right] - \left[\frac{kT}{JS(S+1)} \right]$$

The best fit (assuming $zJ = 0$) of the experimental data to Eq. (1) yielded $J = -0.09 \text{ cm}^{-1}$, $g = 2.05$, $R = 5.0 \times 10^{-5}$ for **1**, $J = -0.33 \text{ cm}^{-1}$, $g = 2.13$, $R = 4.0 \times 10^{-5}$ for **3**, the agreement factor defined as $R = \sum [(\chi_M)_{\text{obsd}}] - [(\chi_M)_{\text{cacld}}]^2 / [(\chi_M)_{\text{obsd}}]^2$.

4. Conclusion

In this paper, four new complexes **1–4** constructed by 5-ferrocene-1,3-benzenedicarboxylic acid and accessorial ligands dpa or

phen with metal ions Co(II) or Zn(II) have been reported. The deliberate design and selection of the ligands is very useful to prepare the complexes with desired architecture and properties. The subtle difference of the subsidiary ligands dpa and phen as well as the coordination models of L result in substantial structural difference: complexes **1** and **2** are 1D helix chains, while **3** and **4** are 1D linear chains. Moreover, hydrogen-bond and π - π stacking interaction play very important role in the construction of supramolecular architectures, which contribute to increasing the knowledge of self-assembly processes and supramolecular self-organization. The magnetic behavior of complexes **1** and **3** were investigated and exhibited antiferromagnetic interactions. Further investigation on the thermal properties of complexes **1–4** shows that all complexes are stable enough until to 300 °C.

Acknowledgements

We gratefully acknowledge financial support from the National Natural Science Foundation of China (20771094, 20671083), the Science and Technology Key Task of Henan Province (0524270061) and the China Postdoctoral Science Foundation (20070410877).

Appendix A. Supplementary material

CCDC 687273, 663361, 687272 and 663362 contains the supplementary crystallographic data for **1**, **2**, **3** and **4**. These data can be obtained free of charge from The Cambridge Crystallographic Data Centre via http://www.ccdc.cam.ac.uk/data_request/cif. Supplementary data associated with this article can be found, in the online version, at doi:10.1016/j.jorgchem.2008.07.034.

References

- [1] J.M. Lehn, *Supramolecular Chemistry – Concepts and Perspectives*, VCH, Weinheim, 1995.
- [2] (a) Q.B. Bo, Z.X. Sun, G.L. Song, F. Li, G.X. Sun, *J. Inorg. Organomet. Polym.* 17 (2007) 615; (b) S.Q. Zang, Y. Su, Y.Z. Li, Z.P. Ni, Q.J. Meng, *Inorg. Chem.* 45 (2006) 174; (c) S. Sailaja, M.V. Rajasekharan, *Inorg. Chem.* 39 (2000) 4586; (d) A. Erxleben, *Inorg. Chem.* 40 (2001) 412; (e) T.D. Owens, f.J. Hollander, A.G. Oliver, J.A. Ellman, *J. Am. Chem. Soc.* 123 (2001) 1539; (f) Y. Ma, Z.B. Han, Y.K. He, L.G. Yang, *Chem. Commun.* 40 (2007) 4107; (g) S.D. Reid, A.J. Blake, C. Wilson, J.B. Love, *Inorg. Chem.* 45 (2006) 636; (h) R.H. Wang, L.J. Xu, X.S. Li, Y.M. Li, Q. Shi, Z.Y. Zhou, M.C. Hong, A.S.C. Chan, *Eur. J. Inorg. Chem.* (2004) 1595.
- [3] (a) X.M. Chen, G.-F. Liu, *Chem. Eur. J.* (2002) 811; (b) Y.G. Li, N. Hao, Y. Lu, E.B. Wang, Z.H. Kang, C.W. Hu, *Inorg. Chem.* 42 (2003) 3119; (c) Y.G. Li, H. Zhang, E.B. Wang, N. Hao, C.W. Hu, Y. Yan, D. Halld, *New J. Chem.* 26 (2002) 1619; (d) Y. Lu, E.B. Wang, M. Yuan, G.Y. Luan, Y.G. Li, H. Zhang, C.W. Hu, Y. Yao, Y. Qin, Y. Chen, *J. Chem. Soc., Dalton Trans.* (2002) 3029.
- [4] T.J. Kealy, P.L. Pauson, *Nature* 168 (1951) 1039.
- [5] (a) R.D.A. Hudson, *J. Organomet. Chem.* 637–639 (2001) 47; (b) C.J. Fang, C.Y. Duan, D. Guo, C. He, Q.J. Meng, Z.M. Wang, C.H. Yan, *Chem. Commun.* (2001) 2540; (c) P.D. Beer, D.K. Smith, *Prog. Inorg. Chem.* 46 (1997) 1; (d) Z.H. Wang, K.C. Chen, H. Tian, *Chem. Lett.* 5 (1999) 423; (e) B. Bildstein, M. Schweiger, H. Angleitner, H. Kopacka, K. Wurst, K.H. Ongania, M. Fontani, P. Zanello, *Organomet.* 18 (1999) 4286; (f) C.J. Fang, C.Y. Duan, D. Guo, C. He, Q.J. Meng, Z.M. Wang, C.H. Yan, *Chem. Commun.* (2001) 2540; (g) G. Li, Y.L. Song, H.W. Hou, L.K. Li, Y.T. Fan, Y. Zhu, X.R. Meng, L.W. Mi, *Inorg. Chem.* 42 (2003) 913.
- [6] (a) M.R. Churchill, Y.J. Li, D. Nalewajek, P.M. Schaber, J. Dorfman, *Inorg. Chem.* 24 (1985) 2684; (b) S.K.C. Kumara, S. Nagabrahmanandachari, K. Raghuraman, *J. Organomet. Chem.* 587 (1999) 132; (c) V. Chandrasekhar, S. Nagendran, S. Bansal, A.W. Cordes, A. Vij, *Organomet.* 21 (2002) 3297; (d) V. Chandrasekhar, S. Nagendran, S. Bansal, M.A. Kozee, D.R. Powell, *Angew. Chem., Int. Ed.* 39 (2000) 1833;

- (e) H.W. Hou, L.K. Li, G. Li, Y.T. Fan, Y. Zhu, *Inorg. Chem.* 42 (2003) 3501;
(f) S.M. Lee, K.K. Cheung, W.T. Wong, *J. Organomet. Chem.* 506 (1996) 77;
(g) A.L. Abuhijleh, C. Woods, *J. Chem. Soc., Dalton Trans.* 7 (1992) 1249.
- [7] (a) G.L. Zheng, J.F. Ma, Z.M. Su, L.K. Yan, J. Yang, Y.Y. Li, J.F. Liu, *Angew. Chem., Int. Ed. Eng.* 43 (2004) 2409;
(b) X.R. Meng, H.W. Hou, G. Li, B.X. Ye, T.Z. Ge, Y.T. Fan, Y. Zhu, H. Sakiyama, *J. Organomet. Chem.* 689 (2004) 1218;
(c) D. Guo, H. Mo, C.Y. Duan, F. Lu, Q.J. Meng, *J. Chem. Soc., Dalton Trans.* (2002) 2593;
(d) S.D. Christie, S. Subramanian, L.K. Thompson, M.J. Zaworotko, *J. Chem. Soc., Chem. Commun.* (1994) 2563;
(e) X.R. Meng, G. Li, H.W. Hou, H.Y. Han, Y.T. Fan, Y. Zhu, C.X. Du, *J. Organomet. Chem.* 679 (2003) 153;
(f) Y.Y. Yang, W.T. Wong, *Chem. Commun.* (2002) 2716;
(g) D. Guo, B.G. Zhang, C.Y. Duan, X. Cao, Q.J. Meng, *J. Chem. Soc., Dalton Trans.* (2003) 282;
(h) M. Kondo, R. Shinagawa, M. Miyazawa, M.K. Kabir, Y. Irie, T. Horiba, T. Naito, K. Maeda, S. Utsuno, F. Uchida, *Dalton Trans.* (2003) 515.
- [8] (a) G. Li, H.W. Hou, L.K. Li, X.R. Meng, Y.T. Fan, Y. Zhu, *Inorg. Chem.* 42 (2003) 4995;
(b) G. Li, H.W. Hou, Z.F. Li, X.R. Meng, Y.T. Fan, *New J. Chem.* 28 (2004) 1595;
(c) H.W. Hou, L.K. Li, Y. Zhu, Y.T. Fan, Y.Q. Qiao, *Inorg. Chem.* 43 (2004) 4767;
(d) L.K. Li, Y.L. Song, H.W. Hou, Y.T. Fan, Y. Zhu, *Eur. J. Inorg. Chem.* 16 (2005) 3238;
(e) L.K. Li, J.P. Li, H.W. Hou, Y.T. Fan, Y. Zhu, *Inorg. Chim. Acta* 359 (2006) 3139.
- [9] G.M. Sheldrick, *SHELXL93*, University of Göttingen, Germany, 1993.
- [10] S.G. Baca, I.G. Filippova, C. Ambrus, M. Gdaniec, Y.A. Simonov, N. Gerbeleu, O.A. Gherco, S. Decurtins, *Eur. J. Inorg. Chem.* 15 (2005) 3118.
- [11] Z. Wang, H.H. Zhang, Y.P. Chen, C.C. Huang, R.Q. Sun, Y.N. Cao, X.H. Yu, *J. Solid State Chem.* 179 (2006) 1536.
- [12] F.A. Cotton, L.R. Fallvello, A.H. Reid, J.H. Tocher, *J. Organomet. Chem.* 319 (1987) 87.
- [13] G. Li, Z.F. Li, H.W. Hou, X.R. Meng, Y.T. Fan, W.H. Chen, *J. Mol. Struct.* 694 (2004) 179.
- [14] B.L. Wu, D.Q. Yuan, F.L. Jiang, L. Han, B.Y. Lou, C.P. Liu, M.C. Hong, *Eur. J. Inorg. Chem.* 7 (2005) 1303.